Pergamon

Geochimica et Cosmochimica Acta, Vol. 67, No. 19, pp. 3773–3783, 2003

0016-7037/03 $30.00 + .00

doi:10.1016/S0016-7037(00)00170-4

Nitrogen isotopic composition of macromolecular organic matter in interplanetary dust particles

JÉRÔME ALÉON,[1,*] FRANÇOIS ROBERT,[2] MARC CHAUSSIDON,[3] and BERNARD MARTY[3,4]

[1]University of California Los Angeles, Department of Earth and Space Sciences, 595 Charles Young Drive, Los Angeles, CA 90095-1567, USA
[2]Muséum National d'Histoire Naturelle, Laboratoire de Minéralogie, CNRS-URA 736, 61 rue Buffon, 75005 Paris, France
[3]Centre de Recherches Pétrographiques et Géochimiques-CNRS, 15 rue Notre Dame des Pauvres, BP 20, 54501 Vandoeuvre-lès-Nancy, France
[4]Ecole Nationale Supérieure de Géologie-INPL, Rue du Doyen Marcel Roubault, BP 40, 54501 Vandoeuvre-lès-Nancy, France

(*Received May* 8, 2002; *accepted in revised form March* 3, 2003)

Abstract—Nitrogen concentrations and isotopic compositions were measured by ion microprobe scanning imaging in two interplanetary dust particles L2021 K1 and L2036 E22, in which imaging of D/H and C/H ratios has previously evidenced the presence of D-rich macromolecular organic components. High nitrogen concentrations of 10–20 wt% and $\delta^{15}N$ values up to +400‰ are observed in these D-rich macromolecular components. The previous study of D/H and C/H ratios has revealed three different D-rich macromolecular phases. The one previously ascribed to macromolecular organic matter akin the insoluble organic matter (IOM) from carbonaceous chondrites is enriched in nitrogen by one order of magnitude compared to the carbonaceous chondrite IOM, although its isotopic composition is still similar to what is known from Renazzo ($\delta^{15}N = +208‰$).

The correlation observed in macromolecular organic material between the D- and ^{15}N-excesses suggests that the latter originate probably from chemical reactions typical of the cold interstellar medium. These interstellar materials preserved to some extent in IDPs are therefore macromolecular organic components with various aliphaticity and aromaticity. They are heavily N-heterosubstituted as shown by their high nitrogen concentrations >10 wt%. They have high D/H ratios $>10^{-3}$ and $\delta^{15}N$ values $\geq +400‰$. In L2021 K1 a mixture is observed at the micron scale between interstellar and chondritic-like organic phases. This indicates that some IDPs contain organic materials processed at various heliocentric distances in a turbulent nebula. Comparison with observation in comets suggests that these molecules may be cometary macromolecules. A correlation is observed between the D/H ratios and $\delta^{15}N$ values of macromolecular organic matter from IDPs, meteorites, the Earth and of major nebular reservoirs. This suggests that most macromolecular organic matter in the inner solar system was probably issued from interstellar precursors and further processed in the protosolar nebula.

1. INTRODUCTION

Interplanetary dust particles (IDPs) are usually thought to be produced by asteroidal collisions or cometary activity (e.g., Brownlee, 1985). During their journey towards the sun, a fraction of them crosses the Earth's orbit and can be collected in the stratosphere by NASA's stratospheric airplanes (e.g., Brownlee, 1985). A subset of carbon-rich, porous and fragile particles with chondritic bulk chemistry and anhydrous mineralogy presents D/H ratios that reach the lowest values measured spectroscopically in molecules from cold molecular clouds or hot molecular cloud cores (Messenger, 2000). These high D/H ratios, relative to chondritic ratios, are associated to organic phases (Keller et al., 2000; Aléon et al., 2001), which likely correspond to several distinct condensed organic phases based on their D/H and C/H ratios (Aléon et al., 2001). Nitrogen isotopic ratios measured in these particles (Messenger, 2000) range up to $\delta^{15}N \sim +500‰$, $\delta^{15}N$ being the deviation relative to the Earth atmosphere ($^{15}N/^{14}N = 1/272$) expressed in per mil. In addition, organic nitrogen has been detected in the carbonaceous matrix of ^{15}N-rich IDPs (e.g., Keller et al., 1997). It has thus been proposed that ^{15}N-rich nitrogen is bounded to organic phases, so that the ^{15}N-excesses might be remnants of interstellar chemistry (e.g., Messenger, 2000). However no clear correlation has yet been evidenced with D/H ratios (Messenger and Walker, 1997) and the processes that could be responsible for such a ^{15}N enrichment in the interstellar medium (ISM) remain poorly known (Terzieva and Herbst, 2000; Charnley and Rodgers, 2002). Therefore the association of high $\delta^{15}N$ values with organic phases of interstellar origin remains to be demonstrated. Furthermore, several complications arise from (i) the evidence of organic matter likely processed within the solar nebula in close association with more D-rich phases (Aléon et al., 2001) and (ii) the presence of extremely high $\delta^{15}N$ values in ~100 nm areas (e.g., $\delta^{15}N \sim +1200‰$, Floss and Stadermann, 2002), pointing possibly to several distinct carriers of N.

This study reports elemental and isotopic imaging of N content and $^{15}N/^{14}N$ ratios in two deuterium-rich IDPs, using a Cameca IMS 1270 ion microprobe. These two IDPs, L2036 E22 and L2021 K1 (hereafter referred to as E22 and K1), show evidence for the presence of at least 3 deuterium-rich organic phases of interstellar origin with C/H ratio ranging from ~0.8 to 3.0 and D/H ratio ranging from 250×10^{-6} to 1880×10^{-6} (Aléon et al., 2001). The determination of the microscale dis-

* Author to whom correspondence should be addressed, at Centre de Recherches Pétrographiques et Géochimiques-CNRS, 15 rue Notre Dame des Pauvres, BP 20, 54501 Vandoeuvre-lès-Nancy, France (aleon@crpg.cnrs-nancy.fr).

tributions of nitrogen concentration and isotopic composition in the three D-rich organic components observed in these 2 IDPs provides new insights into the origin and chemical history of IDPs organic components and allows adequate comparison with meteoritic macromolecules.

2. ANALYTICAL METHODS

2.1. Samples

Sample description and mounting were detailed in Aléon et al. (2001). For ion microprobe analysis the samples were embedded in a clean gold foil. Distributions of Si, C, O and H indicate that silicon oil residues of the collection medium, often considered as organic contaminants in IDPs, are not detected during ion probe analysis (Aléon et al., 2001). Before analysis, the samples were kept under vacuum at 3×10^{-8} Torr during 20 h and heated at ~100°C during 7 h to remove possible atmospheric contamination. To be able to relate the present N measurements with the D/H ratios measured in these IDPs during previous analytical sessions, it is necessary to ensure that previous ion microprobe sputtering did not remove the components of interest. The sputtering is estimated to be less than 70 nm (K1) and 200 nm (E22), which is lower than but close to the size of usual organic units in IDPs (from 0.3 μm to 1 μm, Flynn et al., 1998). SEM (scanning electron microscopy) examination of the particles before and after analysis shows that the latter estimate is typically the grain size of the finest material in these two IDPs. Other carbonaceous components in IDPs include 100 nm thick grain coatings. Given their thickness they are likely to be mostly undistinguished from surrounding organic units. These coatings are made of poorly graphitized amorphous carbon (e.g., Wopenka, 1988) and may correspond to graphitized organic phases. No distinction is thus made here with large condensed organic units. Therefore, carbon was imaged as C^- (10 cycles of 5 s) and compared with the carbon images from the hydrogen analyses to monitor which grains are still present and which were eroded during the first analyses (Figs. 1a,b). In E22, the finest grains are eroded but larger grains corresponding to the deuterium-rich regions are still present after the nitrogen analysis. In K1, one area corresponding to the deuterium-rich component OM2 (Aléon et al., 2001, Table 1 and section 2.2 for a summary) has not been identified but the second one is still present, together with the carbon-rich end-member OM1 (Aléon et al., 2001 and Table 1). Six of the deuterium-rich organic grains from K1 have been identified in both data sets (Fig. 1).

2.2. Organic Components Previously Identified in K1 and E22

From the study of the C/H and D/H ratios in these two particles (Aléon et al., 2001), the hydrogen was inferred to be distributed between a hydrated component (in K1) and a mixture of organic components. Organic mixing end members were labeled OM1, OM2 and OM3 (Fig. 5 in Aléon et al., 2001, Table 1). OM1, with a D/H ratio of $\sim 250 \times 10^{-6}$ and a C/H ratio ~1.5 was inferred to be similar to the macromolecular organic matter of carbonaceous chondrites. OM2 has a D/H ratio of $\sim 1.5 \times 10^{-3}$ and a C/H ratio ~0.8. It was ascribed to a dominantly aliphatic condensed phase, highly heterosubstituted. Finally OM3 is the most D-rich (D/H $\sim 1.9 \times 10^{-3}$) material, it is highly condensed and dominantly aromatic (C/H ~ 3.0). D-rich areas in K1 were found to represent a mixture of OM2 with OM1, the dominant organic phase, whereas OM3 seems a dominant organic constituent of E22, mixed in one area with OM2. The primary goal of the present study is to determine if these D-rich phases also show ^{15}N excesses rather than searching a general correlation between N and H isotopes.

2.3. Nitrogen Isotopes

Nitrogen isotopes were measured by scanning ion imaging at high mass resolution. A Cs^+ primary beam of ~1.5 μm and ~5 pA was rastered on the sample area to be analyzed and for each position of the beam, the ion intensities were measured using an electron multiplier (EM). Images (256 × 256 pixels) were computed by associating these intensities to the position of the beam on the sample. The spatial resolution is thus given by the size of the primary beam. N isotopes were measured as $^{12}C^{14}N^-$ (Fig. 1c) and $^{12}C^{15}N^-$ due to the low ion yield of N^-. A ~7000 mass resolving power is used to separate interferences from $^{10}B^{16}O$, $^{13}C^{12}CH$ and $^{11}B^{16}O$, $^{13}C^{14}N$ at mass 26 and 27, respectively. Each measurement consisted of 40 cycles with counting times per cycle of 3 s for $C^{14}N$ and 30 s for $C^{15}N$. Counting rates in E22 were $\sim 1.2 \times 10^4$ and ~55 counts per second (cps) for $C^{14}N$ and $C^{15}N$, respectively and were $\sim 6.6 \times 10^3$ and ~25 cps in K1. No dead time, drift and detector background corrections were applied because they were estimated to amount to less than a few ‰. Matrix effects for nitrogen isotopes were investigated without image acquisition using standards of kerogens of type I and III and a mixture of olivine plus type III kerogen. Type I kerogens are less mature and more aliphatic than type III kerogens, which have an aromaticity close to that of macromolecular organic matter in carbonaceous chondrites (Gardinier et al., 2000). Matrix effects remain below 5‰ (Table 2). Thus the type III kerogen standard of known $^{15}N/^{14}N$ ratio and known N concentration (Mahakam delta IFP nb 48055, Table 3) was systematically used as the internal standard during isotopic imaging. For this purpose grains of ~30 μm size of this kerogen were mounted onto clean gold foils, similarly to the IDPs. Isotopic ratios are given below in delta notation relative to the air $\delta^{15}N = ([^{12}C^{15}N/^{12}C^{14}N_{sample}]/[^{15}N/^{14}N_{air}] - 1) \times 1000$, where $^{15}N/^{14}N_{air} = 1/272$. Typical accuracy and reproducibility on 20 to 30 μm standard grains are ~5‰. Precision at the micron scale depends mostly on the size and N content of the investigated area. The errors given in Tables 4 and 5 are thus 1σ errors based on the counting statistics.

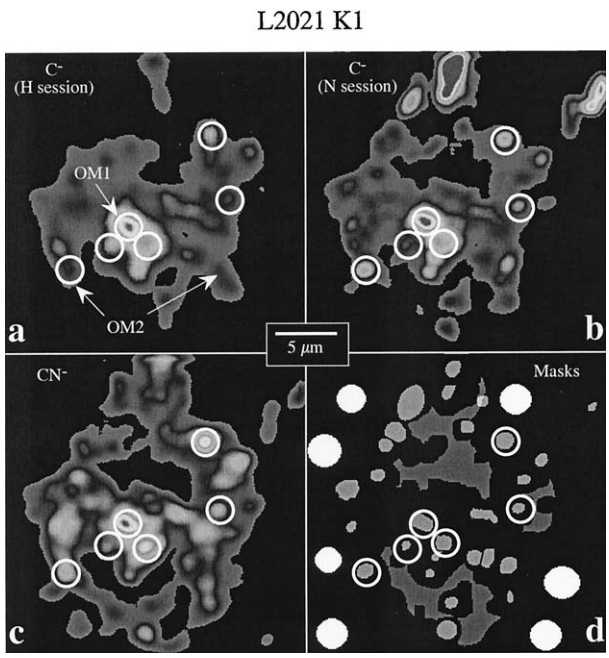

Fig. 1. Ion images of IDP L2021 K1. (a) C^- image acquired during the hydrogen isotopes analytical session (February 2000) (Fig. 2f in Aléon et al., 2001). (b) C^- image acquired during the nitrogen isotopes analytical session (May 2001). (c) CN^- image acquired during the same analytical session as b. (d) Masks corresponding to the areas of Table 4; light gray masks correspond to N, C and CN areas (see text), dark gray masks are O areas (see text) and white masks surrounding the particle are areas used for the determination of the background (see text). White circles show the D-rich regions that were identified in both analytical sessions. The intensity scale was linearly adapted in (a), (b) and (c) to obtain similar grayscale range for easy comparison.

2.4. Nitrogen Concentrations

To report the nitrogen concentration of solid organic compounds, a calibration was established (Fig. 2) by measuring the CN^-/C^- ratios

Table 1. Summary of organic areas observed in Aléon et al. (2001).

Area	C/H	σ C/H	D/H (10^{-6})	σ D/H (10^{-6})	Inferred informations on organic chemistry
C1 in K1 [OM1]	1.51	0.17	253	18	Condensed, similar to carbonaceous chondrites IOM[a]
D7 in K1 [OM2]	1.03	0.12	1480	104	Condensed, dominantly aliphatic, heterosubstituted
D8 in K1 [OM2]	0.78	0.09	1510	116	Same material as D7 [OM2]
D1 in K1	1.16	0.13	1010	42	Mixture of OM1 and OM2
D2 in K1	0.96	0.11	1150	87	Mixture of OM1 and OM2
D3 in K1	1	0.12	1110	61	Mixture of OM1 and OM2
D4 in K1	1.38	0.16	478	28	Mixture of OM1 and OM2
D5 in K1	1	0.11	1120	48	Mixture of OM1 and OM2
D6 in K1	1.21	0.14	528	27	Mixture of OM1 and OM2
D1 in E22 [OM3]	2.94	0.32	1880	112	Highly condensed, dominantly aromatic
D2 in E22	1.40	0.16	1670	120	Mixture of OM2 and OM3

[a] IOM = insoluble organic matter.

(by spot analysis, collection on a Faraday cup and 10-s counting time for each ion) in several macromolecular organic phases of known nitrogen concentration (Table 3). The studied standards range from synthetic polymers (azulmic acid) to highly graphitized natural macromolecules (anthracite) so that the N concentration can be determined in various macromolecules from IDPs, including grains or grain mantles usually described as poorly graphitized carbon. A positive correlation between CN^-/C^- ratios and N concentrations is observed between the various standards (Fig. 2). In a logarithmic plot, this correlation has a slope one indicating that it is a linear correlation. This linear correlation indicates that the emission of CN^- is proportional to the product of the C and N concentrations in the sample. This is similar to what has been observed in metals (Sugiura, 1998) and diamonds (Hauri et al., 2002). The shift between these correlations corresponds to matrix effects between metals, diamonds and solid organic phases. Note that the CN^-/C^- ratios are independent of the primary intensity as shown by similar values obtained with 5 pA, 0.1 nA and 1 nA primary beams (Table 3), which allows intercalibration between spot analysis and imaging. Given possible micron size heterogeneity and small matrix effects, the reproducibility of our calibration is about ± 50% relative, over 2 orders of magnitude. Measurements previously published are in good agreement with the present; calibration within a factor 2 (hydroxybenzotriazole, Zinner et al., 1989; Hoppe et al., 1995; and thymine, Zinner et al., 1989). Despite measuring N as CN^- ions is easier in carbonaceous phases, CN^- ions can also be used to measure trace nitrogen in noncarbonaceous phases by ion microprobe such as in metals (Sugiura, 1998) and silicates (Hashizume et al., 2000). Therefore relative variations of the C^-/CN^- ratio is a reliable proxy of relative variations of 1/N (e.g., Fig. 3).

2.5. Image Processing

Since the spatial resolution is limited by the primary beam size, all the IDP components smaller than 1.5 μm appear in the images as 1.5 μm areas (or "grains"). Grain contours (hereafter referred to as "masks") were extracted from the images by adapted thresholds. Given that the relative intensities of C^- and CN^- can vary in the grains due to (1) submicron mixing between different phases and/or (2) variable N concentration in a given phase and/or (3) true grain size below 1.5 μm, several images were used to minimize the probability to miss any specific phase of the IDPs. Therefore, the masks were defined from $C^{14}N^-$, C^- and O^- images but also from computed images of the C^-/CN^- ratio (C/CN image) and of the $\delta^{15}N$ value ($\delta^{15}N$ image). Taking into account that O and Si are strongly correlated in the studied IDPs (Aléon et al., 2001), inorganic components were defined in K1 using an image of O-rich and C-poor areas computed by subtracting a mask of all C-rich regions to a mask of the O-rich regions (image [OsubC]). These areas have average C^- intensity far below 1.5 counts per pixel, which is the lowest C^- intensity in a mask defined from a carbonaceous region. In E22, O-rich areas overlap strongly with C-rich areas, so that nitrogen in O-rich areas might come preferentially from organic components in some cases. Therefore, by analogy with K1, only areas with less than 1.5 counts per pixel of C^- are considered to represent inorganic components. Masks (and corresponding grains) defined from these various images are labeled N ($\delta^{15}N$ image), CN (C/CN image), C (C^- image) and O (O^- image in E22, [OsubC] image in K1). Within each mask of a grain, intensities of $C^{15}N^-$, $C^{14}N^-$ and C^- have been extracted from the raw images and $\delta^{15}N$ and $C^-/C^{14}N^-$ ratio have been calculated from these intensities. Most of the carbonaceous grains are defined by several masks (e.g., in K1 grain N1 is the same as CN3 and C4). They have thus been reported only once in Tables 4 and 5.

An estimate of potential contamination (mount + instrument) in each particle has been determined by defining several masks of areas in the gold mount surrounding the IDP (e.g., Fig. 1d). $\delta^{15}N$ and $C^-/C^{14}N^-$ ratio have been calculated within these masks labeled Bgd for "Background." Their average $C^-/C^{14}N^-$ ratios and $\delta^{15}N$ are, respectively, 0.021 ± 0.004 and −30 ± 32‰ for E22 (Table 4) and 0.03 ± 0.01 and +56 ± 62‰ for K1 (Table 5). Both are consistent with terrestrial nitrogen either adsorbed from the air onto the sample surface or initially present in the gold foil.

Finally, using data and masks from Aléon et al. (2001), $\delta^{15}N$ and D/H ratios can be obtained for the various areas recognized within the IDPs in the course of the two studies (Fig. 1).

3. RESULTS

3.1. Approach Used to Study the Distribution of N and C in the Two IDPs

Despite the fact that N atoms can only be detected as CN^- ions by ion microprobe, variations in N concentrations can be evidenced both in carbonaceous and non carbonaceous phases. In components unambiguously recognized as organic carbonaceous phases on the basis of their C^- intensities and C/H ratios (Aléon et al., 2001), the calibration from Figure 2 gives directly N concentrations from the CN^-/C^- ratios and this calibration is valid for graphite and more complex carbonaceous matter. In the case of non carbonaceous phases such as silicates, the N emissivity as CN^- drastically depends on the amount of trace

Table 2. Instrumental mass fractionation and matrix effects for N isotopes.

Standard	IMF (‰)	Sigma (‰)
Kerogen type I	−30.3	1.9
Kerogen type III	−34.2	1.6
Kerogen type III + olivine	−31.7	2.3
Kerogen type III (imaging)	−16.7	4.8

Table 3. Standards of condensed organic matter used for nitrogen concentration calibration.

Name	Type	CN^-/C^-	N ppm	Primary current
Mahakam Delta 48055	Type III Kerogen	0.20–0.43[a]	13300	5 pA
Mahakam Delta 48055	Type III Kerogen	0.24–0.38	13300	0.09–0.15 nA
AcideAzulmique	Oxidized azulmic acid[b]	8.65–16.00	365000	0.09–1 nA
SIU-DGC-Res	Resinite concentrate from coal	0.08–0.14	4000	0.15–1 nA
DonH8	Anthracite	0.22	10700	1nA

[a] Determined by image processing.
[b] The azulmic acid standard has been stored about 30 yr in air (Beaumont, personal communication) and is now heavily oxidized. Given that the C/N ratio measured by energy-dispersive X-ray spectroscopy (EDS, C/N = 1.19 ± 0.06)) is equal to that determined by conventional technique (C/N = 1.16 ± 0.05), the N concentration was estimated from the EDS analysis to be 36 ± 5 wt%.

C present and the relationship between CN^-/C^- ratios and N concentrations cannot be easily calibrated. However in this latter case relative variations of the C^-/CN^- ratios do reflect variations of 1/N concentrations and thus can be used with $\delta^{15}N$ values to trace mixing relationships between various components.

3.2. IDP L2036 E22

In E22, the C^-/CN^- ratios and $\delta^{15}N$ values range from 0.10 to 0.32 and from −137‰ to +424‰, respectively (Table 4, Fig. 3a). The $\delta^{15}N$ values increase linearly with the C^-/CN^- ratio, which indicates a binary mixing between a component having a low C^- intensity, a low C^-/CN^- ratio and a $\delta^{15}N$ value ~0‰ and another component having a high C^- intensity, a high C^-/CN^- ratio and a $\delta^{15}N$ value ≥ +400‰. The characteristics of the low C^-/CN^- end member are close to those determined for inorganic nitrogen in gold or atmospheric contamination (see above, Table 4, Fig. 3a). The high C^-/CN^- end member corresponds to an indigenous carbonaceous component having a high $\delta^{15}N$ value. This end member is identified from the ion images (Fig. 4) to be the previously named OM3 organic component. Therefore its N concentration can be determined using the calibration line of condensed organic materials (Fig. 2) and is estimated to be 16 ± 8 wt% (Table 6).

Table 4. Nitrogen isotopes and C^-/CN^- ratios in L2036E22.

Area	C^-/CN^-	$\delta^{15}N$ (‰)	C (counts/pix)	Comment[a]
O7	0.11 ± 0.04	114 ± 72	0.4	I
O5	0.10 ± 0.02	−138 ± 75	0.6	I
O6	0.12 ± 0.04	136 ± 62	1.1	I
O8	0.12 ± 0.03	236 ± 78	1.5	I(?)
C1	0.19 ± 0.02	34 ± 28	3.4	O
O4	0.17 ± 0.01	182 ± 34	5.1	O
O10	0.32 ± 0.03	340 ± 33	5.6	O
O1	0.22 ± 0.03	93 ± 36	5.8	O
C2	0.12 ± 0.01	116 ± 13	6.0	O
C3	0.13 ± 0.01	162 ± 17	6.6	O
C5/D2[b]	0.24 ± 0.02	424 ± 23	8.0	O
O2	0.26 ± 0.04	184 ± 40	8.4	O
C4/D1[b]	0.22 ± 0.01	383 ± 23	22.4	O
B(1–4)[c]	0.021 ± 0.004	−30 ± 32	0.04	B

[a] Dominant N source; I = inorganic, O = organic, B = background.
[b] Areas identified in Aléon et al. (2001).
[c] Average of four areas in Au surrounding the IDP.

3.3. IDP L2021 K1

In K1, the C^-/CN^- ratios and $\delta^{15}N$ values range from 0.07 to 3.28 and from −230‰ to +520‰, respectively (Table 5). With the possible exception of areas N7 and C14 (Table 5), the C^-/CN^- ratios and $\delta^{15}N$ values of all the different C-rich areas which can be identified in K1 are roughly inscribed within a triangle in Figure 3b. These variations in concentration and isotopic composition can be explained by the intricate presence of at least 3 different N-bearing components in K1: (1) a C-rich component having a high C^-/CN^- ratio and a $\delta^{15}N$ value

Table 5. Nitrogen isotopes and C^-/CN^- ratios in L2021K1.

Area	C^-/CN^-	$\delta^{15}N$ (‰)	C (counts/pix)	Comment[a]
O5	0.07 ± 0.01	−82 ± 52	0.4	I
O2	0.19 ± 0.01	7 ± 24	0.5	I
O3	0.19 ± 0.01	10 ± 23	0.6	I
N7	0.08 ± 0.03	520 ± 128	0.7	I (?)
N6	0.14 ± 0.02	18 ± 108	1.5	I (?)
CN13	0.43 ± 0.07	2 ± 110	1.8	O
N5	0.15 ± 0.02	54 ± 47	1.9	O
N9	0.14 ± 0.02	415 ± 140	2.1	O
CN4	0.61 ± 0.03	−68 ± 96	2.2	O
N2	0.21 ± 0.03	269 ± 88	2.3	O
C23	0.12 ± 0.01	121 ± 111	2.4	O
C18	0.23 ± 0.02	79 ± 63	2.5	O
C5	0.16 ± 0.03	116 ± 90	2.8	O
C1	0.31 ± 0.03	14 ± 50	2.9	O
C15	0.38 ± 0.02	−64 ± 103	2.9	O
C17	0.18 ± 0.02	76 ± 90	3.8	O
C2	0.25 ± 0.02	102 ± 119	4.0	O
C7/D5[b]	0.25 ± 0.05	132 ± 137	4.0	O
CN6	0.78 ± 0.03	46 ± 72	4.1	O
CN14	0.41 ± 0.04	155 ± 117	4.4	O
C24	0.20 ± 0.03	202 ± 82	4.8	O
C22/D3[b]	0.22 ± 0.03	261 ± 96	5.0	O
C19/D1[b]	0.17 ± 0.02	214 ± 40	5.6	O
C4/D7[b]	0.30 ± 0.02	372 ± 54	6.4	O
C10	0.42 ± 0.07	170 ± 129	6.6	O
N4/D6[b]	0.228 ± 0.003	332 ± 66	7.1	O
C11	0.33 ± 0.02	363 ± 76	8.0	O
CN8/C1[b]	0.32 ± 0.01	208 ± 46	11.8	O
C14	1.53 ± 0.05	−231 ± 83	17.1	O
C25	0.43 ± 0.04	118 ± 93	17.5	O
C16	3.28 ± 0.18	−35 ± 72	40.9	O
B (1–7)[c]	0.03 ± 0.01	56 ± 62	0.04	B

[a] Dominant N source; I = inorganic, O = organic, B = background.
[b] Areas identified in Aléon et al. (2001).
[c] Average of seven areas in Au surrounding the IDP.

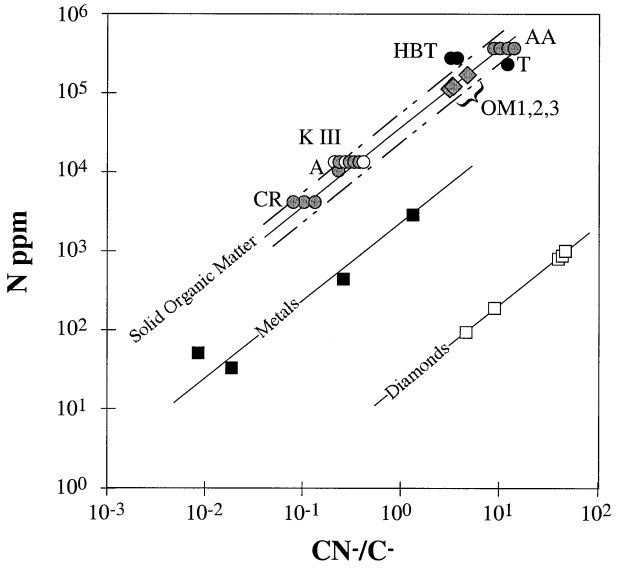

Fig. 2. Calibration curves for the determination of the nitrogen concentration from the CN^-/C^- ratios. White squares are diamonds (Hauri et al., 2002). Black squares are metals (Sugiura, 1998). Circles are solid organic materials. Black circles are from Zinner et al. (1989) and Hoppe et al. (1995), gray circles are organic standards from this study measured by spot analysis and white circles are organic standards from this study measured by ion imaging. Dashed lines show 50% errors. CR = coal resinite; A = anthracite; K III = type III kerogen; AA = azulmic acid; HBT = hydroxybenzotriazole; T = thymine. Gray diamonds are the IDP macromolecular phases OM1, OM2 and OM3.

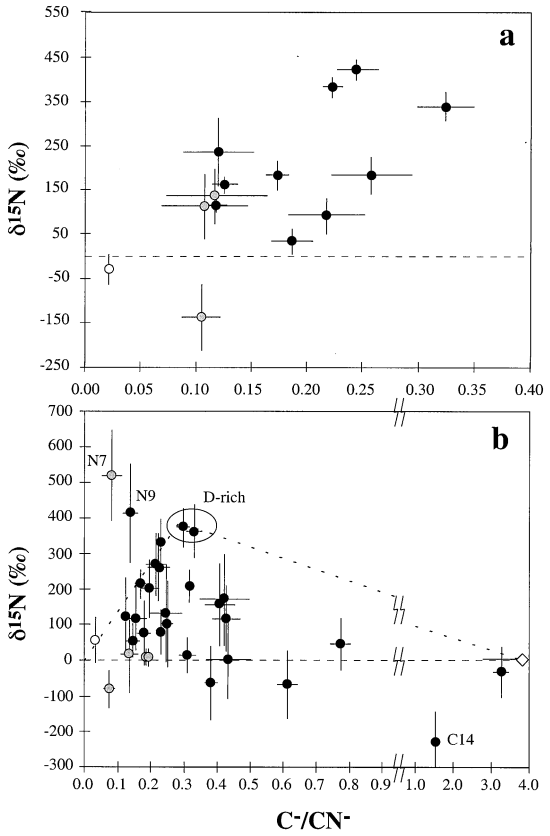

Fig. 3. Nitrogen isotopic composition of micron-sized areas in L2036 E22 (a) and in L2021 K1 (b) as a function of nitrogen concentration uncorrected for relative sensitivity factor. Black dots are carbonaceous areas ($C^- > 1.5$ counts/pixel), gray dots are noncarbonaceous areas ($C^- < 1.5$ counts/pixel), white dots are average background in gold surrounding the particle; see text for the choice of the C^- threshold. The white diamond in (b) is the bulk standard type III kerogen (average of three large fragments) and the dotted lines show the mixing triangle. Areas departing from this triangle are labeled (N7, C14 and possibly N9). Note the scale change on the C^-/CN^- axis between 0.9 and 1.0 in (b).

~0‰ (2) a C- and N-rich component having a low C^-/CN^- ratio and $\delta^{15}N$ values up to +415‰ (3) a C-poor and N-rich component having a low C^-/CN^- ratio and a $\delta^{15}N$ value ~0‰. Intensities of C^- and CN^- and $\delta^{15}N$ values in the latter indicate that this phase is akin the atmospheric-like nitrogen in E22. The C-rich end member having a high N content (C^-/CN^- ~0.3) and a high $\delta^{15}N$ value (~ +400‰) seems similar to that previously identified in E22 and is identified from Figure 1 to be the previously named OM2 organic component. From its CN^-/C^- ratio, its N concentration is 12 ± 6 wt% (Table 6). By contrast, the component having a high C^-/CN^- ratio and a $\delta^{15}N$ value close to 0‰ is only present in K1. Its high C^- intensity points to a N-poor carbonaceous component. Using the calibration line and assuming this carbonaceous component is organic, a 1.2 ± 0.6 wt% nitrogen concentration can be estimated.

Finally, the N7 (and possibly N9) and C14 areas may contain different minor phases whose nature is unclear, a component of high $\delta^{15}N$ value (+520‰, Fig. 3b) and a component of low $\delta^{15}N$ value (−230‰), respectively. Interestingly these components are, respectively, the most ^{15}N-rich and the most ^{15}N-depleted areas in K1. C14 shows the lowest $\delta^{15}N$ value ever observed in an IDP and its high C^- intensity suggest a carbonaceous phase. The large errors associated to these points and the probable mixing with the major components described above prevent further identification.

As a whole, the range of $\delta^{15}N$ values measured in the two present IDPS, from −230‰ to +520‰, is in agreement with previous measurements of IDPs (Stadermann et al., 1989; Messenger, 2000), and the relationships observed at the micron scale between $\delta^{15}N$ values, D/H ratios, H, C and N concentrations allow the characterization of several organic components with nitrogen concentration reaching 10–20 wt% (Table 6).

3.4. Nitrogen Isotopic Composition of Deuterium-Rich Components

A special attention was paid to recognize the deuterium-rich organic components OM1, 2 and 3 (section 2.2, Table 1) identified in our previous D/H-C/H study (Aléon et al., 2001). With the exception of the deuterium-rich area D7 (one of the two areas corresponding to OM2 in Aléon et al., 2001), whose identification from the C image is dubious (Fig. 1), areas corresponding to OM1, 2 and 3 were clearly identified in this study (Figs. 1, 4; and Table 6). They all correspond to C-rich N-rich grains having high $\delta^{15}N$ values and high N concentration. The $\delta^{15}N$ value of the moderately D-rich OM1 is +208 ±

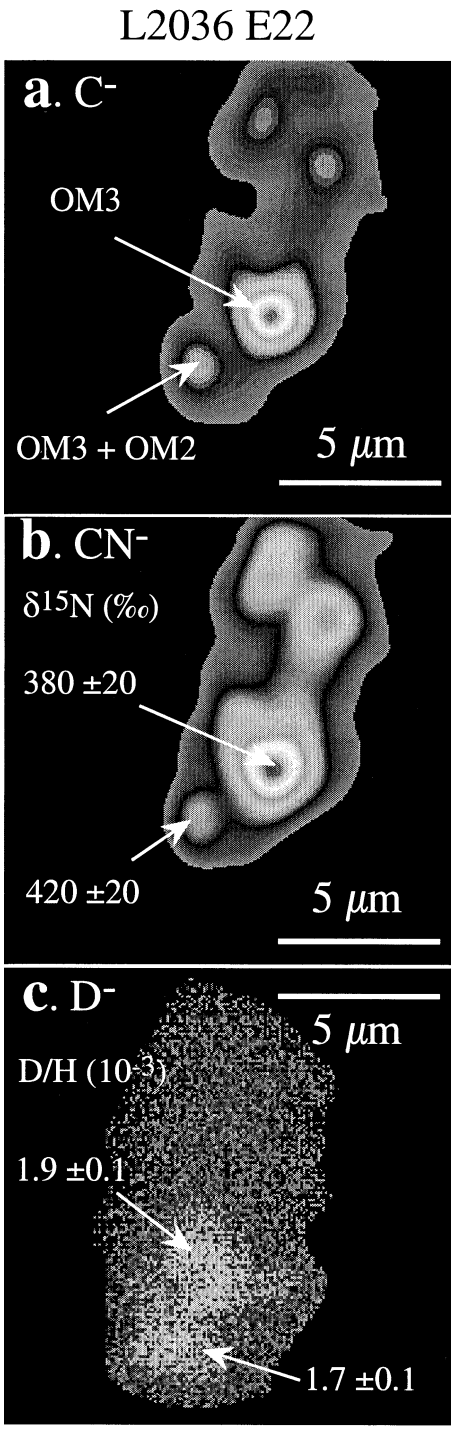

Fig. 4. Ion images of IDP L2036 E22. (a) C^- image. (b) CN^- image. (c) D^- image. $\delta^{15}N$ values (this work) and D/H ratios (Aléon et al., 2001) are reported on (b) and (c) for the organic mixing end members.

46‰ while the $\delta^{15}N$ values of OM2 and OM3, which carry the highest D-excesses, reach +400‰ (Table 6, Fig. 4). The N concentrations are all between 10 and 20 wt% (Table 6), which is an order of magnitude higher than macromolecular insoluble organic matter (IOM) in carbonaceous chondrites (e.g., Robert and Epstein, 1982).

Table 6. N concentrations, $\delta^{15}N$ values, and D/H ratios in D-rich organic regions of K1 and E22.

Grain	D/H (10^{-6})	$\delta^{15}N$ (‰)	N (wt%)
D1 in K1	1010 ± 42	214 ± 40	20 ± 10
D2 in K1[a]	1150 ± 87	—	—
D3 in K1	1110 ± 61	261 ± 96	16 ± 8
D4 in K1[a]	478 ± 28	—	—
D5 in K1	1120 ± 48	132 ± 137	14 ± 7
D6 in K1	528 ± 27	332 ± 66	15 ± 7
D7 in K1 [OM2]	1480 ± 104	372 ± 54	12 ± 6
D8 in K1 [OM2][a]	1510 ± 116	—	—
C1 in K1 [OM1]	253 ± 18	208 ± 46	11 ± 5
D1 in E22 [OM3]	1880 ± 112	383 ± 23	16 ± 8
D2 in E22	1670 ± 120	424 ± 23	15 ± 7

[a] Grains from Aléon et al. (2001) not identified in the present work, probably eroded. D/H ratios are from Aléon et al. (2001).

4. DISCUSSION

4.1. Diverse Indigenous Nitrogen Components in IDPs K1 and E22

From the observation of N abundances and isotopic compositions (Fig. 3), several components can be identified in the two IDPs studied here. These components are summarized in Table 7 and described briefly below.

(1) Most indigenous N corresponds to organic compounds rich in N and with high $\delta^{15}N$ values (e.g., area CN8 and C4 in K1 and C4 in E22, Table 7). This result is in agreement with the observation by Fourier Transform Infra Red spectroscopy of organic nitrogen in the carbonaceous matrix of a ^{15}N-rich IDP (Keller et al., 1997). The direct comparison with D-images indicates that the 3 D-rich organic components previously labeled OM1, OM2 and OM3 (Tables 1 and 6) are such compounds. OM2 and OM3 with D enrichments of 10 and 12 times the terrestrial ratio are probably preserved presolar organic phases. By contrast OM1, with ^{15}N excesses comparable to organic phases of CR chondrites (Robert and Epstein, 1982; Alexander et al., 1998) and D/H ratios comparable to CI, CM chondrites (Robert and Epstein, 1982; Kerridge, 1983), may have been partially reprocessed in the solar nebula (Aléon et al., 2001). Its high N concentration (11 ± 5 wt%) however indicates that this phase is not directly comparable to IOM of carbonaceous chondrites.

(2) Area C16 in K1 corresponds to another carbonaceous component with a $\delta^{15}N$ value and a N concentration compatible with either IOM from carbonaceous chondrites or less likely with terrestrial contamination by a coaly or kerogen-like micrometer-sized particle. Unfortunately the D/H ratio is not available to solve that uncertainty.

(3) Area N7 in K1 (possibly N9 too), shows the presence of a ^{15}N-rich component ($\delta^{15}N = +520‰$). Due to large error bars and low C abundance this value of +520‰ may be a lower limit. Recent observations at the 100 nm scale (Stadermann, 2001; Floss and Stadermann, 2002, 2003) have revealed the presence of small grains with large ^{15}N-excesses reaching +1200‰. Such grains might be related with ^{15}N-rich presolar grains known from meteorites (Si_3N_4, Nittler et al., 1995; type X SiC, e.g., Zinner, 1998; or graphite,

Table 7. Indigenous nitrogen components in IDPs K1 and E22.

Component[a]	D/H[b]	$\delta^{15}N$ (‰)	C^-/CN^-	Possible analogs[c]
CN8 [OM1] (K1)	253×10^{-6}	208 ± 46	0.32	Chondritic IOM? Molecular cloud OM?
C4 [OM2] (K1)	1480×10^{-6}	372 ± 54	0.30	Molecular cloud organic matter
C4 [OM3] (E22)	1880×10^{-6}	383 ± 23	0.22	Molecular cloud organic matter
C14 (K1)	n.l.	-231 ± 83	1.53	Nanodiamonds? Presolar SiC?
N7/N9 (K1)	n.l.	520 ± 128	0.08	Presolar SiC? Si_3N_4? graphite?
C16 (K1)	n.l.	-35 ± 72	3.28	Chondritic IOM? Carbonaceous contamination?

[a] Identified by their area number in Tables 4 and 5.
[b] n.l. = not localized precisely in the H images.
[c] OM = organic matter; IOM = insoluble organic matter.

Amari et al., 1993). Other ^{15}N organic carriers cannot be excluded either.

(4) Area C14 from K1 shows the presence of a C-rich, N-poor component having the lowest $\delta^{15}N$ value (−230‰) observed in an IDP. Similar carbonaceous grains depleted in ^{15}N have been observed in meteorites: mainstream or type Y SiC (Zinner, 1998) or nanodiamonds (Russell et al., 1996).

The presence of OM1, OM2, and phases described above in (2), (3) and (4) in a single noncluster IDP (L2021K1), indicates clearly the presence of a variety of N-bearing species, most of them organic and the other possibly carbonaceous as well. $\delta^{15}N$ values in K1 span almost the total range of $\delta^{15}N$ values observed in cluster IDPs (Messenger, 2000) with the exception of the rare extreme values only detected in submicrometer components of non cluster particles (Stadermann, 2001; Floss and Stadermann, 2002, 2003). The presence of various minor components mixed with abundant ^{15}N-rich and D-rich organic macromolecules likely explains the lack of correlation between H and N isotopes observed in bulk IDPs (e.g., Messenger and Walker, 1997). Since these minor components cannot be identified here, the following discussion is focused on ^{15}N-rich, D-rich organic macromolecules.

4.2. Interstellar Origin of ^{15}N Excesses by Chemical Fractionation

Given the above mentioned absence of correlation between H and N isotopes observed in bulk IDPs (e.g., Messenger and Walker, 1997), a major question is thus to determine the origin of ^{15}N-excesses commonly observed in IDPs. Several origins have been proposed such as (1) nucleosynthesis in massive stars, often considered being the major source of ^{15}N in meteoritic materials via the presence of presolar grains with large isotopic anomalies in the matrices of meteorites (e.g., Zinner, 1998). (2) It has also been proposed that, though not strictly correlated, the ^{15}N excesses are somewhat related to the D excesses observed in IDPs and attributed to molecular cloud chemical fractionation (e.g., Messenger and Walker, 1997). (3) Finally, the spallation production of ^{15}N by cosmic ray exposure needs to be examined. Given that several N-bearing components are likely present in IDPs at a submicrometric scale (see section 4.1), only the origin of ^{15}N-excesses in N-rich organic molecules is addressed here.

First, in-situ production of ^{15}N during spallation by cosmic rays of ^{16}O in IDPs during their journey in the interplanetary medium cannot be a significant source of ^{15}N in IDPs. Indeed, given the abundance of nitrogen (>10 wt%) in the organic material, the amount of spallogenic ^{15}N is limited to a few ‰. This can be estimated assuming (i) a 4π exposure geometry, (ii) a production rate akin to that in lunar soils ($P^{15}N = 5.8 \pm 0.6$ $pg^{15}N/g/Ma$, Mathew and Marti, 2001), (iii) maximum exposure ages of several Ga as proposed from He isotopes (Pepin et al., 2000) and (iv) a maximum abundance of ^{16}O (60 mol% such as in silicates).

The ^{15}N enrichment needs to be discussed with regard to the average interstellar medium (ISM) 4.56 Gy ago (i.e., the protosolar nebula). The D/H ratio of the protosolar nebula is known from the measurement of ^3He in the present-day solar photosphere and from the measurement of the Jovian and Saturnian atmospheric H_2 and is currently estimated to be $21 \pm 5 \times 10^{-6}$ in the major phase H_2 (Geiss and Gloeckler, 1998). The $^{15}N/^{14}N$ ratio of the major nebular reservoir N_2 has been recently determined from the measurement of implanted solar wind in lunar soils ($\delta^{15}N < -240$‰, Hashizume et al., 2000) and from the Jovian atmospheric NH_3 ($\delta^{15}N \sim -375 \pm 82$‰, Owen et al., 2001). From these two estimations the $\delta^{15}N$ value of nebular N_2 adopted here is −350‰.

As shown in section 3.4, N-bearing D-rich macromolecules present in K1 and E22 (Aléon et al., 2001) were identified from both the C^- images and the $\delta^{15}N$ vs. C^-/CN^- distributions. (i) OM3 corresponds to a large (2–3 μm) organic region having a D/H ratio ~100 times the nebular D/H ratio, and a C/H ratio of ~3 indicating a highly condensed phase of probably high aromaticity (Aléon et al., 2001, Fig. 4). The high D/H ratio indicates formation of the organic component by processes occurring at very low temperature (10–50 K), such as ion-molecule reactions, gas-grain reactions or UV photochemistry (e.g., Tielens, 1983; Brown and Millar, 1989; Sandford et al., 2001). These conditions are usually thought to occur in the parent molecular cloud of the solar system (Geiss and Reeves, 1981) but may also have taken place at the surface or in cold regions of the protosolar nebula (Aikawa and Herbst, 1999; Robert, 2002). Since the high $\delta^{15}N$ values observed in E22 are associated to this organic component, it suggests a similar origin for the ^{15}N excesses (Fig. 4). The nitrogen concentration of OM3 (16 ± 8 wt%) is extremely high for a macromolecular organic material. Thus, this material likely contains numerous N heterosubstitutions. (ii) Similar H and

Table 8. Chemical and isotopic composition of macromolecular organic phases in K1 and E22.

Component	C/H	D/H (10^{-6})	δ^{15}N (‰)	N (wt%)	Inferred informations on organic chemistry
OM1	1.51 ± 0.17	253 ± 18	208 ± 46	11 ± 5	Condensed, kerogen-like, N-rich
OM2	1.03 ± 0.12	1480 ± 104	372 ± 54	12 ± 6	Condensed, dominantly aliphatic, N-rich
OM3	2.94 ± 0.32	1880 ± 112	383 ± 23	16 ± 8	Highly condensed, dominantly aromatic, N-rich

N isotopic compositions and concentrations (D/H = 1.5×10^{-3}, δ^{15}N = +400‰, C/H = 0.8 and N~12 wt%) in OM2 indicate similarly a N-rich macromolecular structure but dominantly aliphatic as indicated by the lower C/H ratio (Table 7).

The clear association of high δ^{15}N values with high D/H ratios suggests that the ^{15}N enrichment in OM2 and OM3 is related to some extent to the chemistry that takes place in cold molecular clouds. Ion-molecule reactions have been proposed to cause enrichments of heavy isotopes (Langer et al., 1984), however recent calculations suggests that they cannot be responsible for the δ^{15}N values of +500‰ commonly observed in IDPs (Terzieva and Herbst, 2000). It has been proposed that including gas-grain reactions in models of interstellar chemistry can lead to ^{15}N enrichment of up to a factor 1.8 in the cold interstellar medium (Charnley and Rodgers, 2002). Starting from the nebular δ^{15}N value of −350‰ this would lead to a ~ +300‰ δ^{15}N value consistent with what is observed in OM3 and OM2.

The correlation between ^{15}N and D excesses in organic macromolecules in IDPs indicates that interstellar chemistry is probably responsible for large ^{15}N enrichments in macromolecular organic solids, although more isotopic informations on the source of nitrogen and on the mechanisms of ^{15}N-enrichment are required for a definitive conclusion. Large D-enrichments, high concentrations of N and large ^{15}N-enrichments are probably common characteristics of this type of chemistry (Table 8).

4.3. Modified Interstellar Organic Macromolecules in K1

The OM1 component has a δ^{15}N value ~ +210‰, close to that of IOM from the CR chondrite Renazzo (Robert and Epstein, 1982) and a N concentration ~10 times higher than that of carbonaceous chondrites IOM (Robert and Epstein, 1982; Kerridge, 1983; Alexander et al., 1998) but indistinguishable from that of the rather pristine interstellar component OM2 and OM3 (10 to 20 wt%). Since it has C/H and D/H ratios similar to that of IOM of CI and CM chondrites (Aléon et al., 2001, Table 1) it seems to be a macromolecular component close to that of carbonaceous chondrites but different from IOM of any distinct carbonaceous chondrite group.

The nitrogen isotopic composition of other D-rich grains (Table 6) is within error compatible with that of OM1, OM2 or intermediate between the two. Similarly they have all high N concentrations between 10–20 wt% (Table 6). This is compatible with a mixture between OM1 and OM2 as proposed from the C/H and D/H ratios (Aléon et al., 2001, Table 1). It implies a physical mixture of components with various degree of reprocessing in the solar nebula before their accretion in the L2021 K1 parent body. Such a mixing could occur by large-scale turbulence such as described in recent models of the solar nebula (e.g., Drouart et al., 1999; Hersant et al., 2001) which allow gathering of materials from various heliocentric distances. Such a mixture of pristine interstellar grains with grains reprocessed in the inner regions of the nebula explains both the distribution of organic material observed in IDPs (Aléon et al., 2001, this work) and the distribution of silicates in comets (Bockelée-Morvan et al., 2002).

4.4. Cometary Macromolecules?

Having high nitrogen concentrations (10–20 wt%) the present D-rich refractory organic components show similarities with CHON grains detected by Giotto and Vega in dust from comet Halley (Jessberger et al., 1988; Fomenkova et al., 1994, Table 8). The ^{14}N/^{15}N ratio of HCN in the coma of comet Hale-Bopp is slightly higher than the terrestrial ratio (^{14}N/^{15}N = 323 ± 46 or in δ-notation δ^{15}N ~ −160 ± 120‰, Jewitt et al., 1997), intermediate between the terrestrial value and the −350‰ value of the protosolar nebula. HCN is often considered to be a molecule initially present as a component of cometary ices (e.g., Irvine et al., 1996; Biver et al., 1997; Wright et al., 1998). By contrast, the CN radical is inferred to originate partly from the ices, partly from the degradation of N-rich polymers close to the perihelia (Woodney et al., 2002). The recent observation of ^{15}N excesses in the CN radical in comets Hale-Bopp and C2000 WM1 (LINEAR) (C. Arpigny, personal communication) suggests thus the presence of ^{15}N-rich macromolecular organic compounds in cometary nuclei. OM1, OM2 and OM3 may be such cometary macromolecular grains. In addition the morphology of L2021 K1 (large Mg-rich crystals (~5 μm) with adhering micron to submicron grains among which the D-rich carbonaceous components) and L2036 E22 (only micron to submicron grains including the D-rich carbonaceous components) is consistent with the expected properties of cometary dust. In this hypothesis, the N isotopic difference between HCN_{ice} and CN_{grains} is consistent with gas-grain chemical models predicting a large ^{15}N-enrichment in the grains compared to the gas phase (Charnley and Rodgers, 2002). At the temperature of cometary nuclei, the N isotopic exchange is probably negligible, although the exact kinetic rate constants are still to be determined. Therefore, initial isotopic differences between grains and ices inherited from the interstellar or protosolar chemistry are probably preserved in comets and the nitrogen-rich, ^{15}N-rich, D-rich macromolecular organic components OM1, OM2 and OM3 are potentially cometary organic molecules.

4.5. Macromolecular Organic Matter in the Solar System

The observations of large δ^{15}N associated with large D/H ratios typical of cold cloud chemistry in a subset of macromo-

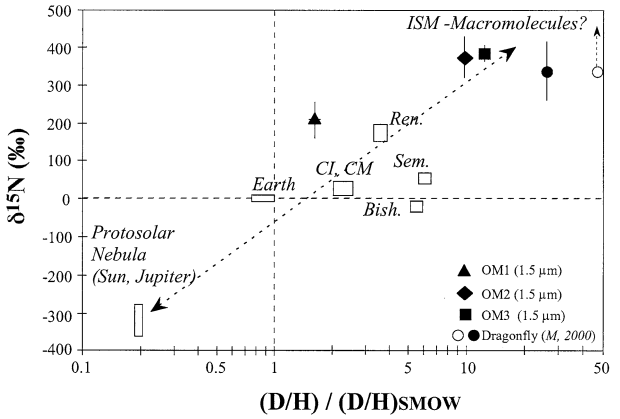

Fig. 5. Hydrogen and nitrogen isotopic composition of identified macromolecular organic matter in K1, E22, in the Renazzo (Ren.) CR carbonaceous chondrite (Robert and Epstein, 1982; Yang and Epstein, 1983; Alexander et al., 1998), in the Bishunpur (Bish.) and Semarkona (Sem.) LL3 ordinary chondrites (McNaughton et al., 1982; Robert et al., 1987; Alexander et al., 1998), in CI and CM carbonaceous chondrites (Robert and Epstein, 1982; Kerridge, 1983) and on Earth, compared with major hydrogen and nitrogen reservoirs of the protosolar nebula (H_2, Geiss and Gloeckler, 1998); N_2 estimated from N in the sun (Hashizume et al., 2000); and from NH_3 in Jupiter atmosphere (Owen et al., 2001). Additional data from the IDP Dragonfly in which the highest D/H ratio corresponding to organic material has been observed (Keller et al., 2000; Messenger, 2000) are also reported: the black dot is the spot analysis of the corresponding IDP fragment and the white dot shows the D/H ratio of the organic area estimated from direct ion imaging (Messenger, 2000). Unfortunately, no estimate of the nitrogen isotopic composition is available for the organic area; the dotted arrow indicates that it is probably higher than that of the spot measurement. Dashed lines show the Standard Mean Ocean Water and Air reference values.

lecular organic compounds in IDPs (OM2, OM3), together with moderate excesses of both D and ^{15}N in another group of macromolecular organic phases having similarities with chondritic components (OM1), suggest that nitrogen and hydrogen isotopes can be used to study the origin and evolution of macromolecular organic matter in the protosolar nebula. A clear trend is visible from Figure 5 between D/H ratio and $\delta^{15}N$ of various macromolecular components in IDPs, chondrites, the Earth and of the major nebular reservoirs H_2 and N_2, these latter being enriched in light H and N isotopes. Intermediate components like terrestrial and chondritic IOM were either (i) issued from interstellar precursors re-equilibrated in the solar system by a wide variety of processes such as organic chemistry, isotopic exchange with water or nebular gas and/or degradation during thermal or aqueous alteration in parent-body or nebular environments or (ii) resulting from the mechanical mixing of submicron organic components of interstellar origin with submicron organic grains formed in the solar nebula. Macromolecules themselves have probably many functional groups with different reactivities. The complexity of this process and the absence of clear knowledge on interstellar precursors preclude any simple modelling, so that the identification and the quantification of the various steps involved in this process remain open questions. The scatter in the intermediate region corresponding to terrestrial and chondritic components may simply result from various mixing proportions, various degrees of isotopic exchange or different degrees of maturation, etc. Because of (i) temperature dependance or (ii) mixing proportions, it is probable that the observed isotopic gradient (Fig. 5) represents a gradient of heliocentric distances. Macromolecular organic matter is by far the most important carbonaceous component in IDPs and meteorites and thus in solar system primitive small bodies such as asteroids and possibly in cometary nuclei. Therefore reprocessed macromolecules of interstellar origin may be a major source of carbon for inner solar system planetesimals in regions where nebular gases such as CO are completely dissipated during planetary accretion and not captured like in giant planets atmospheres and maybe in cometary ices.

5. CONCLUSIONS

This study confirms the observation of macromolecular organic phases in IDPs, issued from a molecular cloud-type chemistry. It has been shown previously, that these organic phases can be dominantly aliphatic or dominantly aromatic (Aléon et al., 2001). It is shown here, that both types of molecules are largely nitrogen heterosubstituted (10–20 wt% N) and enriched in ^{15}N by $\sim +400‰$ relative to the Earth atmosphere.

The observation in IDPs of macromolecules having preserved a pristine interstellar signature and of macromolecules exposed to isotopic exchange with the protosolar nebula gas is probably due to a complex accretionary history of IDPs, whose parent bodies could have sampled organic phases issued from various heliocentric distances in a turbulent nebula.

By comparison with the cometary CHON grains and with isotopic observations in comets, the nitrogen concentration and isotopic composition of the present refractory organic phases suggests that these macromolecules may be cometary and thus that the two IDPs K1 and E22 may be cometary.

When compared to other Solar System objects and to the major H and N reservoirs of the protosolar nebula, the macromolecular organic components from IDPs show a positive correlation between their $\delta^{15}N$ and D/H ratios. This indicates an origin of solar system macromolecules by nebular re-processing of D- and ^{15}N-rich interstellar precursors, in agreement with previous ideas (e.g., Robert and Epstein, 1982; Kerridge, 1983; Yang and Epstein, 1983) and suggests that these macromolecules may be a major source of carbon for the inner solar system planetesimals.

Acknowledgments—Janet Borg and Eric Quirico are thanked for initially providing the IDP samples. We are grateful to Cécile Engrand for her contribution to the study of hydrogen isotopes. The present measurements were possible thanks to the careful maintenance of the IMS 1270 ion microprobe under the responsibility of Denis Mangin and Michel Champenois. Laure Sangely is warmly thanked here for providing several terrestrial standards of macromolecules from her PhD thesis. Valérie Beaumont is thanked for the initial work on the azulmic acid and type III kerogen standard. Discussions with Dominique Bockelée-Morvan and especially with Claude Arpigny were useful and appreciated. We would like to thank careful editorial work by Rainer Wieler and detailed comments and reviews by Frank Stadermann, Thomas Stephan and an anonymous reviewer. This work was supported by the Région Lorraine and by PNP-INSU grants, This is CRPG-CNRS contribution 1623.

Associate editor: R. Wieler

REFERENCES

Aikawa Y. and Herbst E. (1999) Deuterium fractionation in protoplanetary disks. *Astrophys. J.* **526,** 314–326.

Aléon J., Engrand C., Robert F., and Chaussidon M. (2001) Clues to the origin of IDPs from the isotopic study of their H-bearing phases. *Geochim. Cosmochim. Acta* **65,** 4399–4412.

Alexander C. M. O'D., Russell S. S., Arden J. W., Ash R. D., Grady M. M., and Pillinger C. T. (1998) The origin of chondritic macromolecular organic matter: A carbon and nitrogen isotope study. *Meteor. Planet. Sci.* **33,** 603–622.

Amari S., Hoppe P., Zinner E., and Lewis R. (1993) The isotopic compositions and stellar sources of meteoritic graphite grains. *Nature* **365,** 806–809.

Biver N., Bockelée-Morvan D., Colom P., Crovisier J., Davies J. K., Dent W. R. F., Despois D., Gérard E., Lellouch E., Rauer H., Moreno R., and Paupert G. (1997) Evolution of the outgassing of comet Hale-Bopp (C/1995 O1) from radio observations. *Science* **275,** 1915–1918.

Bockelée-Morvan D., Gautier D., Hersant F., Huré J.-M., and Robert F. (2002) Turbulent radial mixing in the solar nebula as the source of crystalline silicates in comets. *Astron. Astrophys.* **384,** 1107–1118.

Brown P. D. and Millar T. J. (1989) Models of the gas–grain interaction—Deuterium chemistry. *Mon. Not. R. Astr. Soc.* **237,** 661–671.

Brownlee D. E. (1985) Cosmic dust: Collection and research. *Annu. Rev. Earth Planet. Sci.* **13,** 147–173.

Charnley S. B. and Rodgers S. D. (2002) The end of interstellar chemistry as the origin of nitrogen in comets and meteorites. *Astrophys. J.* **569,** L133–L137.

Drouart A., Dubrulle B., Gautier D., and Robert F. (1999) Structure and transport in the Solar Nebula from constraints on deuterium enrichment and giant planets formation. *Icarus* **140,** 129–155.

Floss C. and Stadermann F. J. (2002) Nanosims measurements of nitrogen isotopic distributions in IDPs and Renazzo: Uniform ^{15}N enrichment in a chondritic IDP. *Lunar Planet Sci. Conf.* **33,** 1350.

Floss C. and Stadermann F. J. (2003) Complementary carbon, nitrogen and oxygen isotopic imaging of interplanetary dust particles: Presolar grains and an indication of a carbon isotopic anomaly. *Lunar Planet Sci. Conf.* **34,** 1238.

Flynn G. J., Keller L. P., Jacobsen C., and Wirick S. (1998) Carbon mapping and carbon-XANES bonding state measurements on interplanetary dust particles. *Lunar Planet. Sci. Conf.* **29,** 1159.

Fomenkova M. N., Chang S., and Mukhin L. M. (1994) Carbonaceous components in the comet Halley dust. *Geochim. Cosmochim. Acta* **58,** 4503–4512.

Gardinier A., Derenne S., Robert F., Behar F., Largeau C., and Maquet J. (2000) Solid state CP/MAS ^{13}C NMR of the insoluble organic matter of the Orgueil and Murchison meteorites: quantitative study. *Earth Planet. Sci. Lett.* **184,** 9–21.

Geiss J. and Reeves H. (1981) Deuterium in the solar system. *Astron. Astrophys.* **93,** 189–199.

Geiss J. and Gloeckler G. (1998) Abundances of deuterium and helium in the protosolar cloud. *Space Sci. Rev.* **84,** 239–250.

Hashizume K., Chaussidon M., Marty B., and Robert F. (2000) Solar wind record on the moon: Deciphering presolar from planetary nitrogen. *Science* **290,** 1142–1145.

Hauri E. H., Wang J., Pearson D. G., and Bulanova G. P. (2002) Microanalysis of δ^{13}C, δ^{15}N and N abundances in diamonds by secondary ion mass spectrometry. *Chem. Geol.* **185,** 149–163.

Hersant F., Gautier D., and Huré J.-M. (2001) A two dimensional model for the primordial nebula constrained by D/H measurements in the solar system: Implication for the formation of giant planets. *Astrophys. J.* **554,** 391–407.

Hoppe P., Amari S., Zinner E., and Lewis R. (1995) Isotopic compositions of C, N, O, Mg and Si, trace element abundances, and morphologies of single circumstellar graphite grains in four density fractions from the Murchison meteorite. *Geochim. Cosmochim. Acta* **59,** 4029–4056.

Irvine W. M., Bockelée-Morvan D., Lis D. C., Matthews H. E., Biver N., Crovisier J., Davies J. K., Dent W. R. F., Gautier D., Godfrey P. D., Keene J., Lovell A. J., Owen T. C., Phillips T. G., Rauer H., Schloerb F. P., Senay M., and Young K. (1996) Spectroscopic evidence for interstellar ices in comet Hyakutake. *Nature* **383,** 418–420.

Jessberger E. K., Christoforidis A., and Kissel J. (1988) Aspects of the major element composition of Halley's dust. *Nature* **332,** 691–695.

Jewitt D. C., Matthews H. E., Owen T., and Meier R. (1997) Measurements of ^{12}C/^{13}C, ^{14}N/^{15}N and ^{32}S/^{34}S ratios in comet Hale-Bopp (C/1995 O1). *Science* **278,** 90–93.

Keller L. P., Messenger S., Miller M., and Thomas K. L. (1997) Nitrogen speciation in a ^{15}N-enriched interplanetary dust particle. *Lunar Planet. Sci. Conf.* **28,** 707.

Keller L. P., Messenger S., Flynn G. J., Jacobsen C., and Wirick S. (2000) Chemical and petrographic studies of molecular cloud materials preserved in interplanetary dust. *Meteor. Planet. Sci.* **35,** A86–A87.

Kerridge J. F. (1983) Isotopic composition of carbonaceous-chondrite kerogen: Evidence for an interstellar origin of organic matter in meteorites. *Earth Planet. Sci. Lett.* **64,** 186–200.

Langer W. D., Graedel T. E., Frerking M. A., and Armentrout P. B. (1984) Carbon and oxygen isotope fractionation in dense interstellar clouds. *Astrophys. J.* **277,** 581–604.

Mathew K. J. and Marti K. (2001) Lunar nitrogen: Indigenous signature and cosmic-ray production rate. *Earth Planet. Sci. Lett.* **184,** 659–669.

McNaughton N. J., Fallick A. E., and Pillinger C. T. (1982) Deuterium enrichments in type 3 ordinary chondrites. *J. Geophys. Res.* **87,** A297–A302.

Messenger S. (2000) Identification of molecular-cloud material in interplanetary dust particles. *Nature* **404,** 968–971.

Messenger S. R. and Walker R. M. (1997) Evidence for molecular cloud material in meteorites and interplanetary dust. In *Astrophysical Implications of the Laboratory Study of Presolar Materials* (eds. T. J. Bernatowicz and E. Zinner), pp. 545–564. American Institute of Physics.

Nittler L. R., Hoppe P., Alexander C. M. O.'D., et al. (1995) Silicon nitride from supernovae. *Astrophys. J.* **453,** L25–L28.

Owen T., Mahaffy P. R., Niemann H. B., Atreya S., and Wong M. (2001) Protosolar nitrogen. *Astrophys. J.* **553,** L77–L79.

Pepin R. O., Palma R. L., and Schlutter D. J. (2000) Noble gases in interplanetary dust particles, I: The excess helium 3 problem and estimates of the relative fluxes of solar wind and solar energetic particles in interplanetary space. *Meteor. Planet. Sci.* **35,** 495–504.

Robert F. (2002) Water and organic matter D/H ratios in the solar system: A record of an early irradiation of the nebula? *Planet. Space Sci.* **50,** 1227–1234.

Robert F. and Epstein S. (1982) The concentration and isotopic composition of hydrogen, carbon and nitrogen in carbonaceous chondrites. *Geochim. Cosmochim. Acta* **46,** 81–95.

Robert F., Javoy M., Halbout J., Dimon B., and Merlivat L. (1987) Hydrogen isotope abundance in the solar system. Part I: Unequilibrated chondrites. *Geochim. Cosmochim. Acta* **51,** 1787–1805.

Russell S. R., Arden J. W., and Pillinger C. T. (1996) A carbon and nitrogen isotope study of diamond from primitive chondrites. *Meteor. Planet. Sci.* **31,** 345–355.

Sandford S. A., Bernstein M. P., and Dworkin J. P. (2001) Assessment of the interstellar processes leading to deuterium enrichment in meteoritic organics. *Meteor. Planet. Sci.* **36,** 1117–1133.

Stadermann F. J. (2001) Hydrogen, carbon and nitrogen isotopic imaging of sub-micron components from interplanetary dust particles. *Lunar Planet. Sci. Conf.* **32,** 1792.

Stadermann F. J., Walker R. M., and Zinner E. (1989) Ion microprobe measurements of nitrogen and carbon isotopic variations in individual IDPs. *Meteoritics* **24,** A327.

Sugiura N. (1998) Ion probe measurements of carbon and nitrogen in iron meteorites. *Meteor. Planet. Sci.* **33,** 393–409.

Terzieva R. and Herbst E. (2000) The possibility of nitrogen isotopic fractionation in interstellar clouds. *Mon. Not. R. Astron. Soc.* **317,** 563–568.

Tielens A. G. G. M. (1983) Surface chemistry of deuterated molecules. *Astron. Astrophys.* **119,** 177–183.

Woodney L. M., A'Hearn M. F., Schleicher D. G., Farnham T. L., McMullin J. P., Wright M. C. H., Veal J. M., Snyder L. E., de Pater I., Forster J. R., Palmer P., Kuan Y.-J., Williams W. R., Cheung C. C., and Smith B. R. (2002) Morphology of HCN and CN in Comet Hale-Bopp (1995 O1). *Icarus* **157,** 193–204.

Wopenka B. (1988) Raman observations on individual interplanetary dust particles. *Earth Planet. Sci.* **88,** 221–231.

Wright M. C. H., de Pater I., Forster J. R., Palmer P., Snyder L. E., Veal J. M., A'Hearn M. F., Woodney L. M., Jackson W. M., Kuan Y.-J., and Lovell A. J. (1989) Mosaicked images and spectra of J = 1→0 HCN and HCO^+ emission from comet Hale-Bopp (1995 O1). *Astron. J.* **116,** 3018–3028.

Yang J. and Epstein S. (1983) Interstellar organic matter in meteorites. *Geochim. Cosmochim. Acta* **47,** 2199–2216.

Zinner E. (1998) Trends in the study of presolar dust grains from primitive meteorites. *Meteorit. Planet. Sci.* **33,** 549–564.

Zinner E., Tang M., and Anders E. (1989) Interstellar SiC in the Murchison and Murray meteorites: Isotopic composition of Ne, Xe, Si, C and N. *Geochim. Cosmochim. Acta* **53,** 3273–3290.